

4.0 RESULTS AND DISCUSSION

4.1 Introduction

This chapter describes in detail the test results of thermal stability, surface morphology, fire protection performance and bonding strength of the intumescent samples by using TGA, SEM, FESEM, Bunsen burner test, furnace test and Instron microtester as mentioned in the previous chapter. All the sections in this chapter are arranged according to the process of formulation and characterization of the intumescent samples.

4.2 Investigation of Flame Retardant Additives

Based on the literature review in chapter two, flame retardant additives such as polyphosphate, boric acid, tri(3,4-epoxycyclohexylmethyl) phosphate (TECP), urea phosphate tributyl phosphate, guanidine and chlorinated paraffins were used to prepare the intumescent fire protective coatings to protect the underlying substrate in the event of a fire (Rains, 1994; Wang et al., 2009). In this research, the combination of three main environmentally friendly and halogen-free flame retardant additives i.e. (i) ammonium polyphosphate phase II (APP II), (ii) pentaerythritol (PER) and (iii) melamine (MEL) with different composition ratios were adopted. TGA test was conducted to investigate the thermal stability of the selected flame retardant additives.

4.2.1 Thermal Stability of AMP System

Four formulations of AMP systems were studied in this research study i.e. (i) A1, (ii) A2, (iii) A3 and (iv) A4. APP II acts as an acid source, MEL acts as a blowing agent and PER acts as a carbon source. The intumescent coatings which contain APP II will start to decompose when exposed to an accidental fire or heat, commonly into

polymeric phosphoric acid and ammonia (NH_3). Additions of synergetic products like PER and MEL derivatives will significantly improve the flame retardant performance of APP II.

The TGA curves of the four AMP systems showed similar profiles (as shown in Figure 4.1). When the temperature exceeds 215°C , there was a sharp decrease in residual weight.

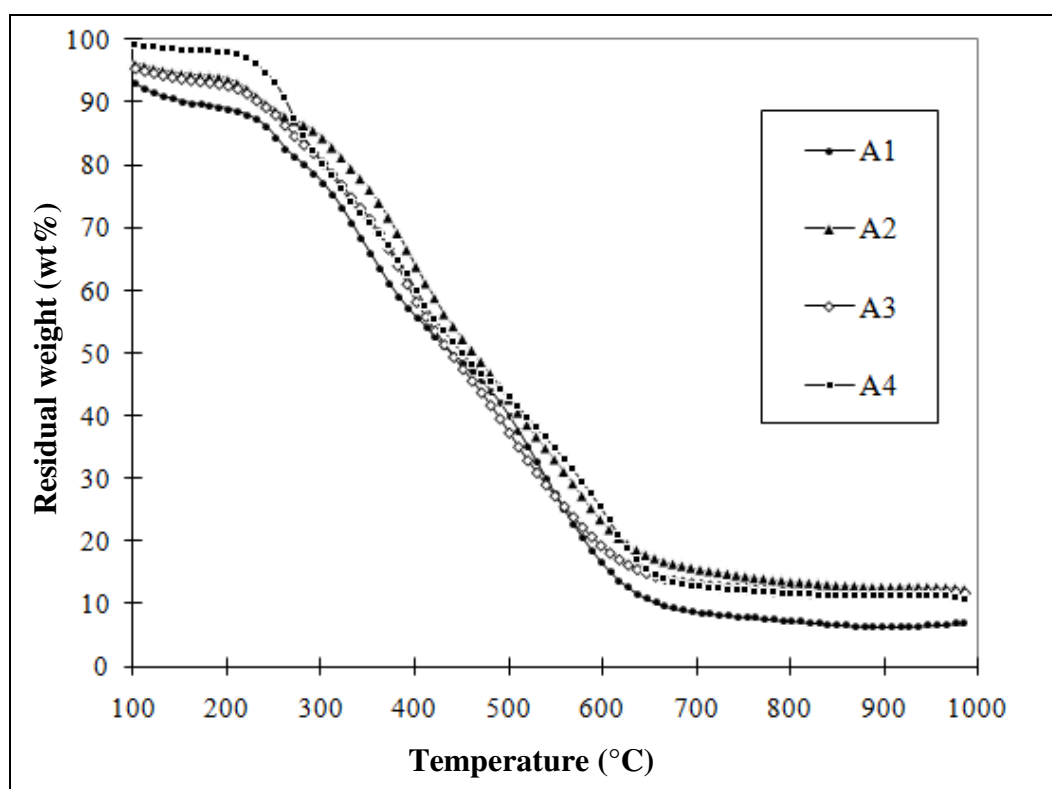


Figure 4.1 TGA curves of the AMP system

The decomposition of all samples occurred between temperatures of 215°C to 640°C . In this study, only the sample with the highest thermal stability was selected and its chemical and physical mechanism studied. The highest residual weight of sample A2 indicated that the formulation had the best anti-oxidation and highest thermal stability under air flow compared to the other samples. The detailed chemical and

physical mechanism of sample A2 is explained based on the decomposition temperature of each flame retardant agent.

The thermal stability characteristics of sample A2 are presented in Table 4.1. The thermal degradation of sample A2 occurs in three main steps: the first step between 215°C and 310°C, corresponding to a residual weight of 90 wt.%. In the first step, 10 wt.% mass loss was due to dehydration and fusion of PER. The first step of degradation can be assigned to the degradation of PER as shown in Figure 4.2.

Table 4.1: Thermal stability of sample A2

		A2
First step	T_{onset} (°C)	215
	T_{end} (°C)	310
	Residual wt. (%) at T_{end}	90
Second step	T_{onset} (°C)	310
	T_{end} (°C)	620
	Residual wt. (%) at T_{end}	20
Third step	T_{onset} (°C)	620
	T_{end} (°C)	1000
	Residual wt. (%) at T_{end}	13

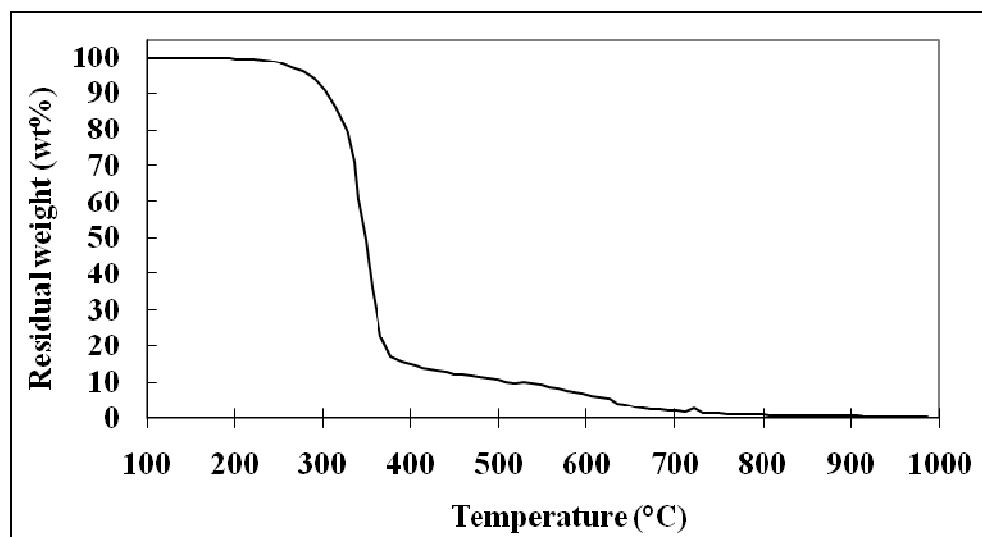


Figure 4.2 TGA curve of pentaerythritol

The second step occurs between 310°C and 600°C corresponding to a residual weight of 20 wt.%. This step may partly correspond to the polyphosphate decomposing to phosphoric acid, ammonia (NH₃) and water (H₂O) resulting in char formation (Bourbigot et al., 1995; Kandola and Horrocks, 1996; Richard et al., 1996). There is also the possibility of polyphosphoric acid formation from phosphoric acid with the release of H₂O vapour and NH₃ from the APP II (Horrocks et al., 2005). In fact, APP II begins to lose NH₃ at a temperature slightly above 300°C (as shown in Figure 4.3), resulting in a highly condensed polyphosphoric acid (Camino et al., 1991). This step also corresponds to the degradation of the coating agent of the APP II derivative, which contains nitrogenous and carbonaceous species.

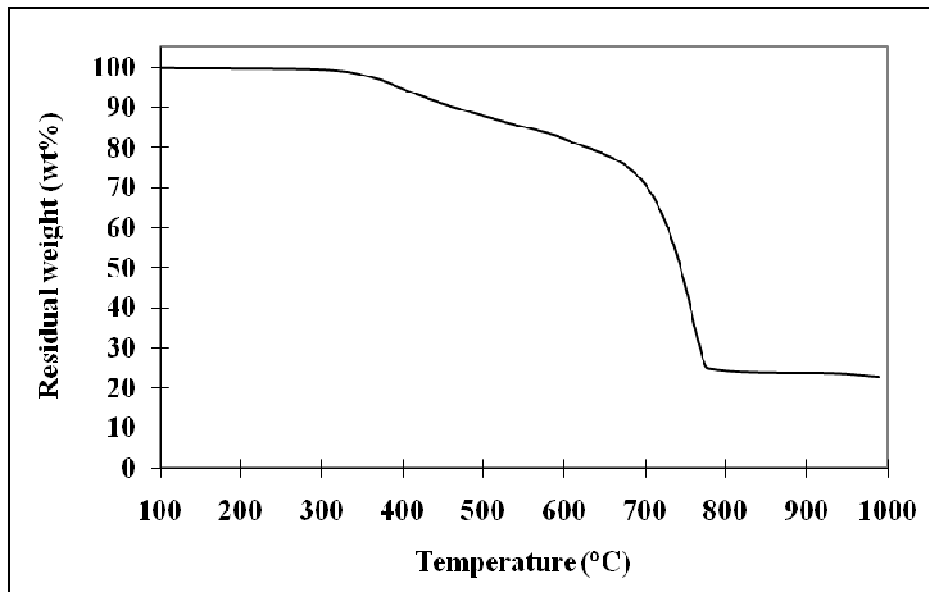


Figure 4.3 TGA curve of ammonium polyphosphate phase II

Then, a thermally stable material is formed that degrades from 600°C up to 800°C in the third step and results in a residue of about 13 wt.%. APP II forms a phosphocarbon structure that is thermally stable. This stabilized residue acts as a protective thermal barrier during the intumescent fire retardancy process. MEL, the third constituent of the intumescent formulation which acts as a blowing agent starts releasing NH₃ at temperature 300°C and this continues up to 400°C as shown in Figure 4.4. As a result, swelling of the intumescent coating takes place.

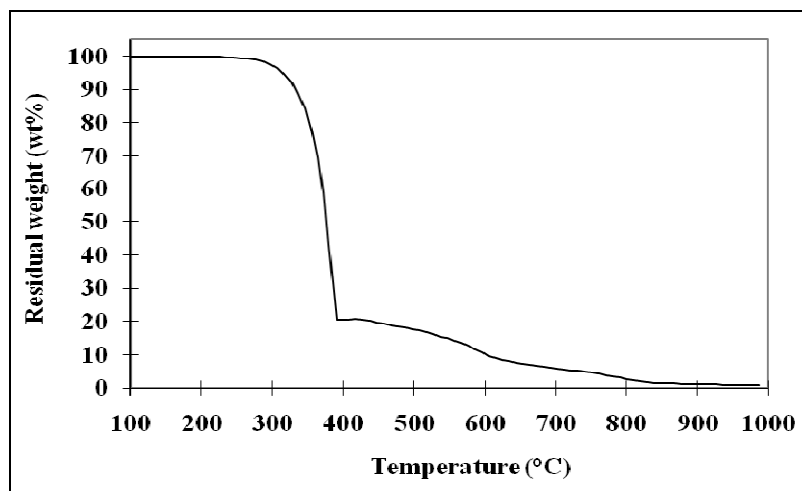


Figure 4.4 TGA curve of melamine

4.3 Investigation of Flame Retardant Fillers

Presently, intumescent coating industries use alumina trihydrate (ATH), titanium dioxide (TiO_2) or magnesium hydroxide $\text{Mg}(\text{OH})_2$ as flame retardant fillers. Particulate fillers can strongly influence the combustion characteristics of intumescent coatings, including its resistance to ignition, and the extent and nature of smoke and toxic gas emission products. This may result from simple dilution of the combustible fuel source, slowing down the diffusion rate of oxygen and flammable pyrolysis products and changing the melt rheology of the coatings, thereby affecting its tendency to drip. However, depending on the nature of the filler, the heat capacity, thermal conductivity and emissivity of the intumescent composition may also change, giving rise to heat transfer and thermal reflectivity effects, which can also slow the rate of burning.

Bellayer and his coworkers (2009) have been investigated the intumescent behaviour of linear low-density polyethylene (LLDPE) containing calcium carbonate (CaCO_3) (chalk) as mineral filler treated by stearic acid. CES is an industrial byproduct containing 95 % CaCO_3 , and its disposal constitutes a serious environmental hazard (Toro et al., 2007). Recycling useful industrial by-products such as CES helps to prevent accumulation of wastes, thus decreasing land pollution. Using an aviculture by-product CES as flame retardant filler in the intumescent coating results in an environmentally friendly invention that not only protects human lives but also preserves the environment. In this experimental work, the thermal stability of CES and commercial CaCO_3 were compared and studied.

4.3.1 Thermal Stability of CES and Calcium Carbonate

In this study, CES as bio-filler was compared with that commercial CaCO_3 filler by TGA test. The TGA curves showed that there are differences in the thermal

decomposition of CES and commercial CaCO_3 as shown in Figure 4.5. Commercial CaCO_3 has only one stage of thermal degradation, whereas CES has two stages (as shown in Table 4.2). For CES, the first stage of thermal degradation occurs between the temperatures of 300°C to 790°C where weight loss is about 7 wt.% due to dehydration of the CES. The second stage which occurred between the temperatures of 790°C to 907°C shows 39 wt.% of mass loss due to the formation of calcium oxide (CaO) and the release of carbon dioxide (CO_2). The thermal degradation of commercial CaCO_3 which occurs between temperatures of 742°C to 850°C shows 53.5 wt.% residual weight. The temperature for 10 wt.% weight loss of CES and commercial CaCO_3 are 810°C and 770°C respectively. Furthermore, CES decomposes completely at about 907°C and the commercial CaCO_3 at around 850°C . Hence, the temperature for complete decomposition of CES is higher than that of commercial CaCO_3 . Moreover, the residue left for CES and commercial CaCO_3 at 1000°C were almost the same, at 53.0 wt.% and 53.5 wt.% respectively. This proves that the CES had better thermal stability compared to commercial CaCO_3 .

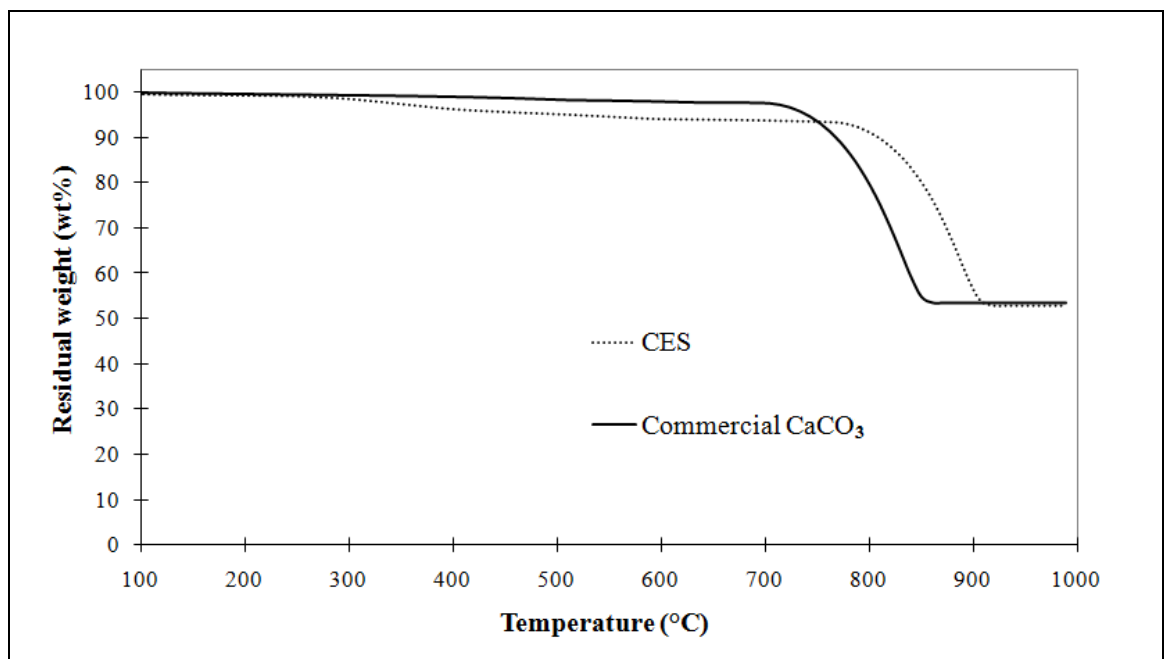


Figure 4.5 TGA curves of chicken eggshell and commercial CaCO_3

Table 4.2: Thermal stability of CES and commercial CaCO₃

		Commercial CaCO ₃	CES
First step	T_{onset} (°C)	742	300
	T_{end} (°C)	850	790
	Residual wt. (%) at T_{end}	53.5	93
Second step	T_{onset} (°C)		790
	T_{end} (°C)		907
	Residual wt. (%) at T_{end}		53.0

4.3.2 Decarbonation and Recarbonation of CES

To study the decarbonation and recarbonation of CES, TGA experiments were carried out under air flow. Mass change measurements were recorded during heating and cooling in the temperature range of 30°C to 1000°C. Results show drastic mass loss at 790°C and mass increase between 480°C and 515°C as shown in Figure 4.6. The mass loss is attributed to the complete decarbonation of CES into CaO and CO₂ (Figure 4.6, Eq. (1)). It can be concluded that CES acts as an additional blowing agent when exposed to temperatures above 790°C. On the other hand, the mass increase is due to the partial recarbonation of CaO during the cooling phases (Figure 4.6, Eq. (2)). The results show that CES as a bio-filler reduces negative impact on the environment due to its ability to absorb CO₂ from the air during partial recarbonation (Bellayer et al., 2009). CES was found to have a direct physical flame retardant action. As the temperature rises, this filler decomposes endothermically and therefore absorbs energy (Hornsby, 2007). Moreover, it releases non-flammable molecules (CO₂), which dilute combustible gases to stop spreading of fire, and also promotes the formation of a protective vitreous layer. Thus CES is a good candidate as a bio-filler due to its availability in bulk quantity, cost effectiveness, excellent fire protection performance as well as having environmentally friendly properties.

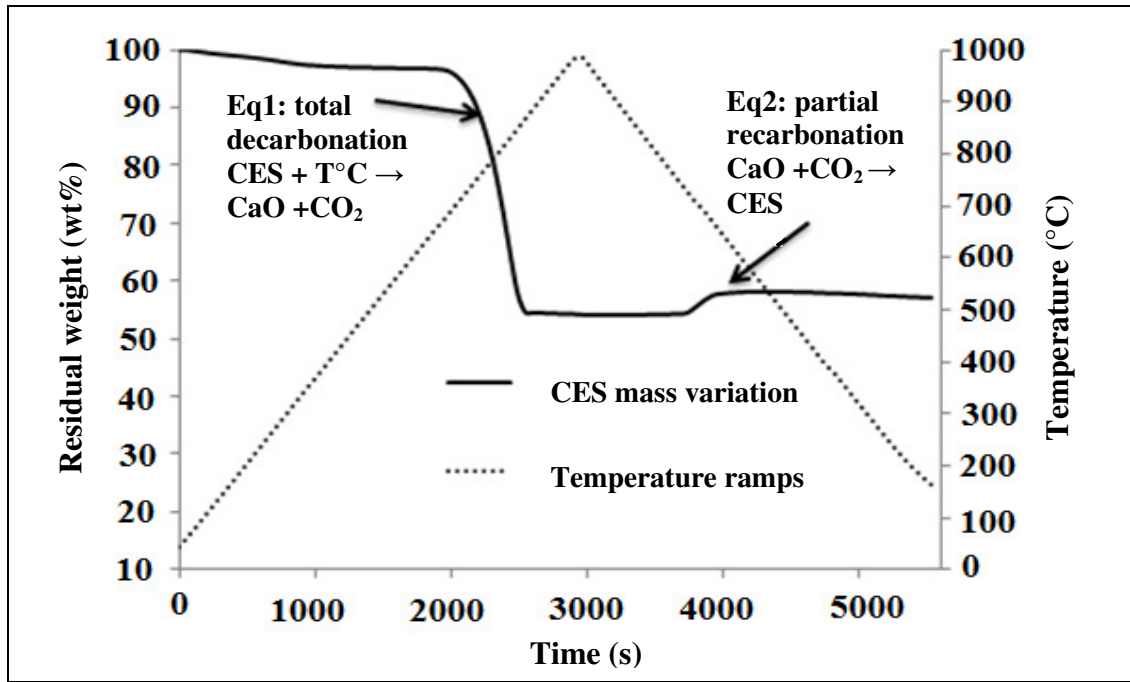


Figure 4.6 TGA graphs of CES at 20°C/min heating and cooling ramp under air flow and chemical changes that occurred during the two ramps

4.4 Fire Protection Test of Intumescent Coatings on Steel

During the Bunsen burner test, the evolution of temperature on the back of the coated steel plate as a function of time was recorded and investigated. The temperatures were measured using a digital thermometer which was connected to a thermocouple on the back of the steel plates coated with the different formulations.

Subsequently, four different samples of each coating system (AMP+SF, AMP+SF+CES and AMP+SF+CES+ER) were tested and the time-temperature curves were plotted. The samples were subjected to a high temperature flame (about 1000°C) using a Bunsen burner. The temperature evolution of a steel plate without protection (Figure 4.7) was also tested as a control for the purpose of comparison.

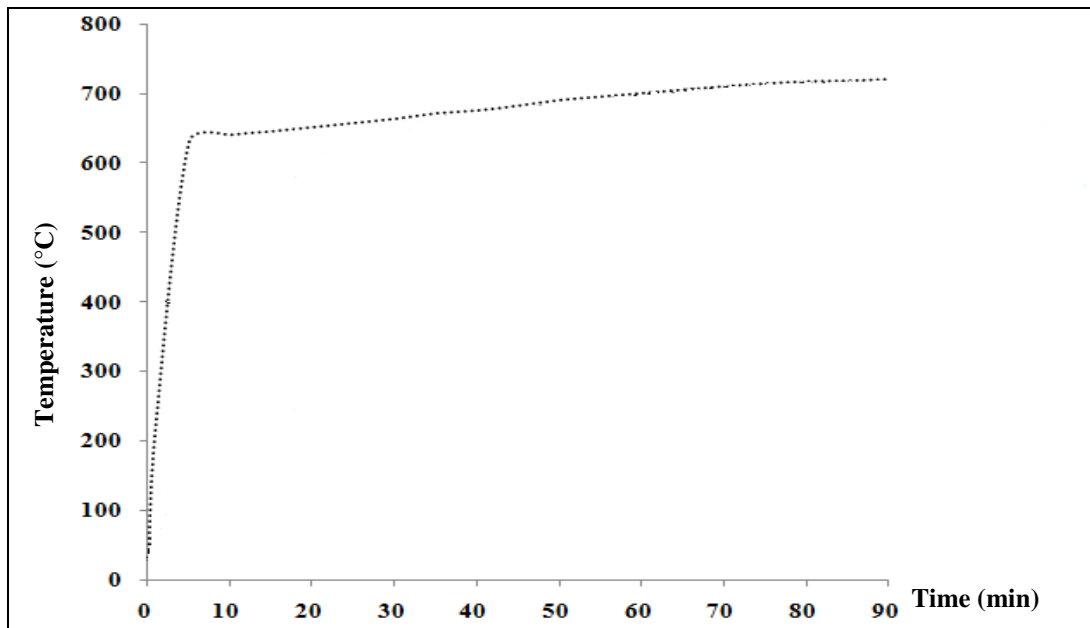


Figure 4.7 The time-temperature curve of uncoated steel plate under fire test

For the AMP coating system, coating formulation A2 which had the highest thermal stability was subjected to the Bunsen burner test. The time-temperature curve of this coating was plotted and the fire protection ability was subsequently compared with a representative of each coating system which had the best fire protection performance in its own category (AMP+SF, AMP+SF+CES and AMP+SF+CES+ER). The purpose of this comparison is to investigate the influence of the addition of (i) SF (ii) combination of SF and CES; and (iii) combination of SF, CES and ER content on the three active flame retardant additives. The results are discussed in terms of thermal stability, fire protection performance, sticking ability and surface morphology of the coatings.

The formation of char and the reaction of the intumescent coatings in a fire were investigated. Besides that, the furnace test was carried out to investigate the behavior of protected and unprotected steel plates in this study. The best sample from the AMP+SF+CES coating system was applied onto a 200 mm x 200 mm x 3 mm steel plate to obtain a 1.2 ± 0.1 mm thick coating and then compared with the unprotected steel plate under furnace test. The furnace temperature was controlled to closely follow the

Eurocode parametric standard temperature-time curve as described in Eurocode 1 part 1-2 (EC1, 2002).

4.4.1 AMP+SF Coating System

Four types of AMP+SF coating systems were studied i.e. (i) B1, (ii) B2, (iii) B3 and (iv) B4. During the Bunsen burner test, the temperature of the back side of the steel plate was plotted as a function of time (Figure 4.8) and the influence of SF content on the fire protection of coatings was evaluated.

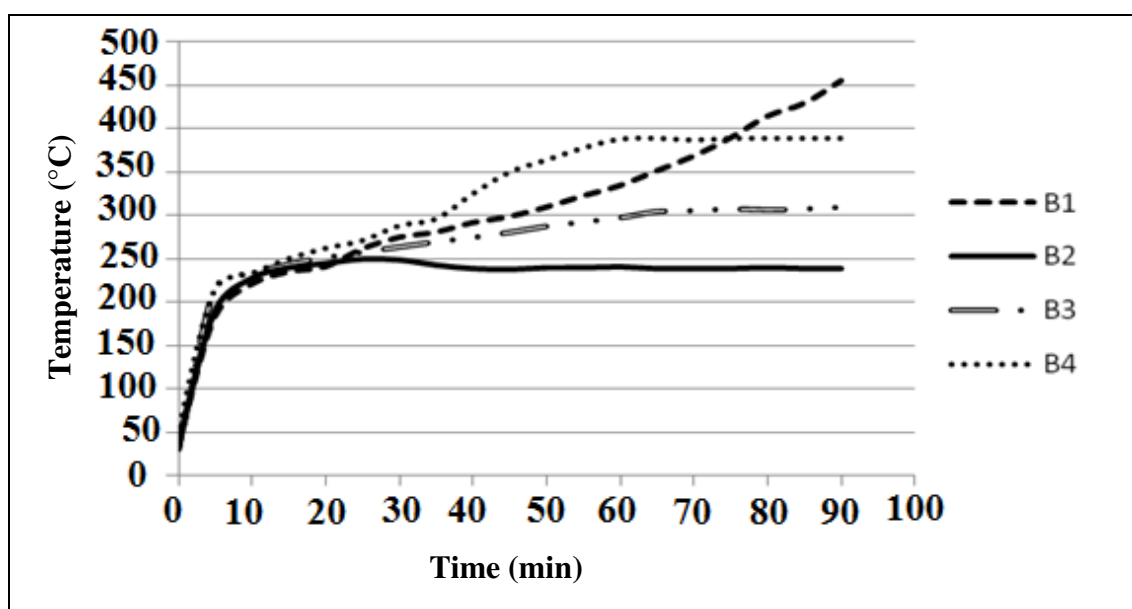


Figure 4.8 Evolution of temperature on the back of the steel plates of AMP+SF system

Table 4.3: Char thickness and equilibrium temperature of AMP+SF coating system

Sample	Thickness of char layer (mm)	Equilibrium temperature of coating (°C)
B1	*	> critical temperature
B2	24.4	240
B3	20.6	305
B4	18.1	388

* The coating did not adhere to the steel plate during Bunsen burner test

During the first 10 minutes, there was not much difference in the temperature of each coating. The shape of the temperature profiles was almost similar for all the coatings

between the temperatures of 30°C to 250°C. Twenty minutes into the test, the temperature profiles of the 4 systems started to differ from each other. The temperature of sample B1 increased rapidly after 20 minutes of the fire test. This phenomenon is due to insufficient content of SF binder that holds the formation of char layer on the steel plate. As a result, some of the char detached from the plate during testing. Poor adhesion of coating B1 to the steel plate led to its inability to protect the steel plate during fire.

The temperature of sample B2 reached an equilibrium value at about 240°C after 33 minutes of fire testing and remained almost unchanged thereafter. Sample B2 showed improvement in fire protection performance compared to sample B1 which reached a maximum temperature of 455°C after exposure to 90 minutes of fire. The addition of 10 wt.% of SF as a binder in sample B2 permits continuous adhesion between the coating and steel plate, providing longer-lasting fire protection.

The experimental results showed that the equilibrium temperatures of B2, B3 and B4 were 240°C, 305°C and 388°C respectively. This indicates that the increase in SF content leads to the increase in the equilibrium temperature of the coatings. The increase of SF content hinders the mechanism of intumescence which in turn reduces the fire protection ability of the coating. The addition of 10 wt.% of SF was found to be optimal for effective fire protection as it enables adhesion of the coating on the steel plate without compromising on the performance of the coating.

The thickness of the char layer of each system was measured after burning (Table 4.3) and it was found that there was a correlation between thickness of the char layer and equilibrium temperature. The thicker the char layer, the lower the equilibrium

temperature. This shows that the thickness of the char layer correlates with the fire protection performance of the coating.

4.4.2 AMP+SF+CES Coating System

Four formulations of AMP+SF+CES coating systems were studied i.e. (i) C1, (ii) C2, (iii) C3 and (iv) C4. The temperature of the back of the coated steel plate was plotted as a function of time (Figure 4.9) and the influence of CES content on the fire protection of the coatings was evaluated. The temperature profiles were almost similar for all the coatings. During the first 5 minutes, there was no temperature difference between the coatings, which increased rapidly and attained 176°C. After 18 minutes into the test, the temperature reached an equilibrium value and remained almost unchanged until the end of the test. The experimental results showed that the equilibrium temperature of C1, C2, C3 and C4 were 220°C, 208°C, 183°C and 225°C respectively. This shows that with the increase of CES content, the equilibrium temperature of the coatings decreased, with the exception of sample C4. Sample C3 with 25 wt.% CES content had the best fire protection performance in the Bunsen burner test. Addition of 30 wt.% CES in sample C4 exceeded the optimal content of CES for effective fire protection. This disrupted the mechanism of intumescence which led to reduced fire protection.

The coating with the thickest char layer also had the lowest equilibrium temperature, which was just 183°C (Table 4.4). The equilibrium temperature of sample C3 is the best among all the coating systems.

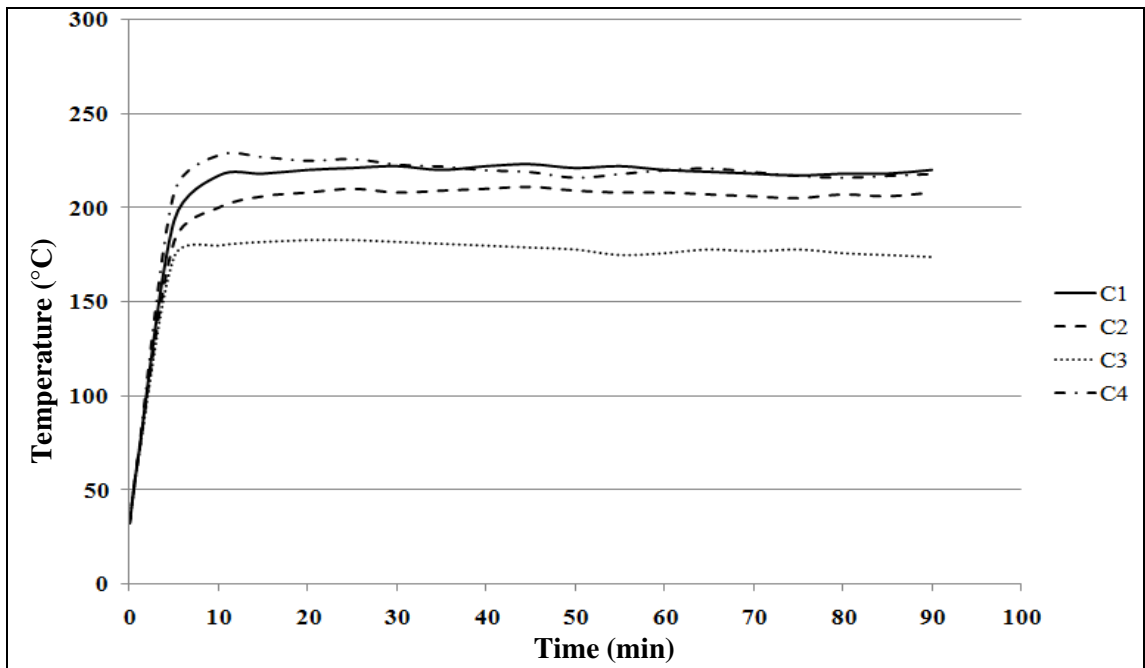


Figure 4.9 Evolution of temperature on the back of the steel plates of AMP+SF+CES system

Table 4.4: Char thickness and equilibrium temperature of AMP+SF+CES coating system

Sample	Thickness of char layer (mm)	Equilibrium temperature of coating (°C)
C1	31.9	220
C2	37.3	208
C3	43.9	183
C4	30.4	225

4.4.3 AMP+SF+CES+ER Coating System

Four formulations of AMP+SF+CES+ER coatings (marked as D1-D4) were studied using the fire protection test. During the test, the temperature of the back of the coated steel plates were plotted as a function of time (as shown in Figure 4.10) and the influence of epoxy content on the fire protection performance of coatings was evaluated. The curves of the temperature profiles were similar for coatings D1, D3 and D4. During the first 5 minutes, there was no difference in temperature for D1, D3 and D4, and the temperature increased rapidly and reached about 200°C. The experimental results showed that the equilibrium temperature of D1, D2, D3 and D4 were 215°C, 210°C, 219°C and 233°C respectively as shown in Table 4.5. Sample

D2 had a relatively lower heating rate during the first 16 minutes and a lower equilibrium temperature than the other coatings. Sample D2 (combination of C3 and 10 wt.% epoxy) showed the best fire protection performance in this system due to its optimal amount of 10 wt.% epoxy binder which resulted in the best chemical and physical reactions during the Bunsen burner test.

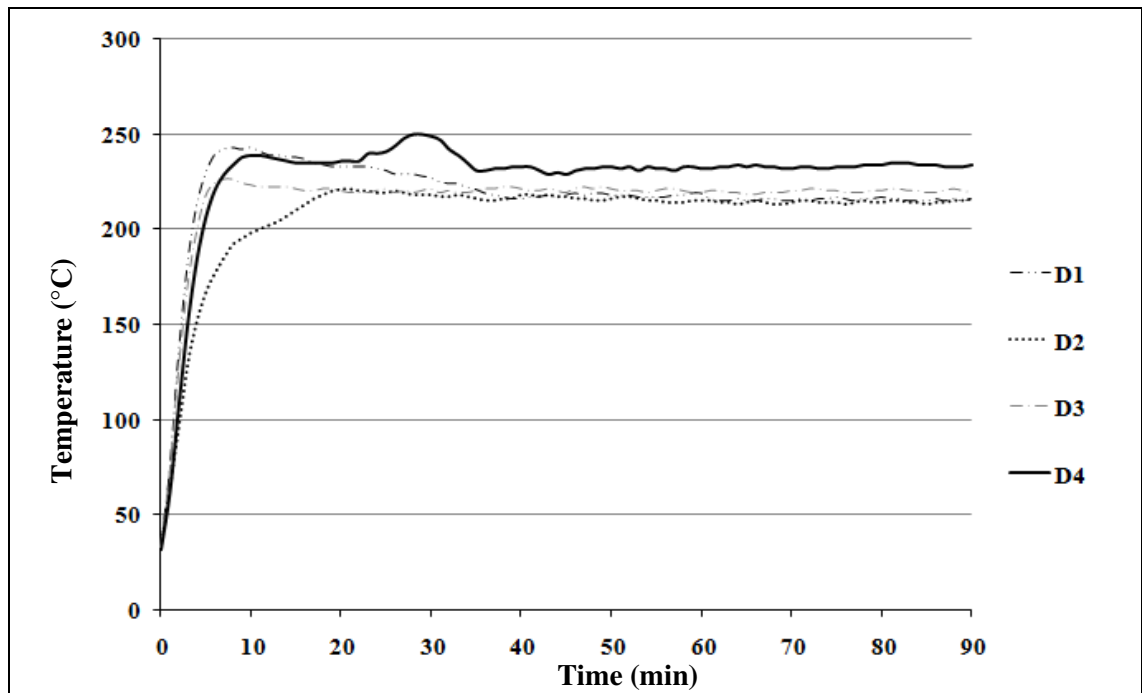


Figure 4.10 Evolution of temperature on the back of the steel plates of AMP+SF+CES+ER system

Table 4.5: Char thickness and equilibrium temperature of AMP+SF+CES+ER system

Sample	Thickness of char layer (mm)	Equilibrium temperature of coating (°C)
D1	24.4	215
D2	28.7	210
D3	20.1	219
D4	18.6	233

4.4.4 Comparison of Intumescent Coating System (A2, B2, C3 and D2)

In this section, the temperature profile of the best formulation from each of the four intumescent coating systems were compared and investigated as shown in Figure 4.11. The four best formulations were chosen and subsequently compared to the bare

steel plate i.e. (i) AMP (A2), (ii) A2 mixed with 10 wt.% SF (B2), (iii) B2 mixed with 25 wt.% CES (C3) and (iv) C3 mixed with 10 wt.% ER (D2).

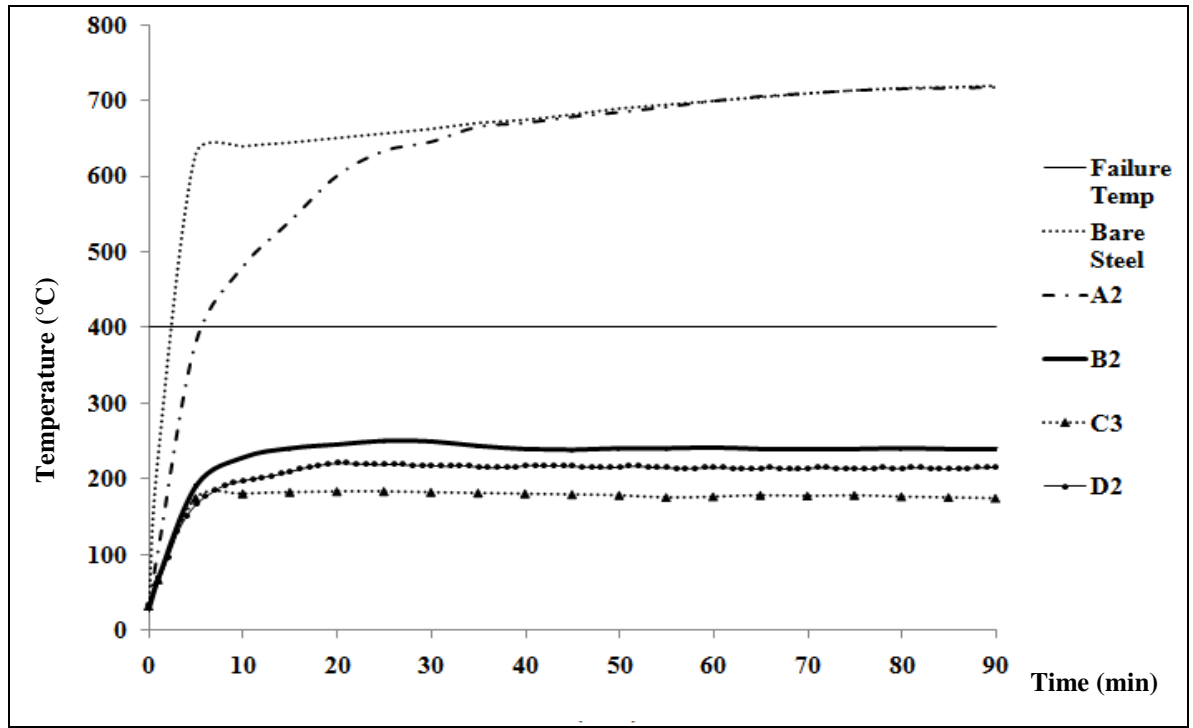


Figure 4.11 Evolution of temperature on the back of the steel plates coated with the best formulations of intumescent coating system

The properties of steel are reduced by 60 % at 400°C, hence this temperature was chosen as the critical temperature (BS5950, 1990). The steel plate coated with AMP formulation (A2) reached the critical temperature in merely 6 minutes. The time-temperature curves of coating samples B2, C3 and D2 showed similar profiles. During the first 5 minutes of fire, there was no temperature difference between the 3 coatings, and the temperature increased rapidly to 182°C. After 15 minutes, the temperature reached equilibrium and remained almost unchanged until 90 minutes of the test. The results of the Bunsen burner test showed that B2, C3 and D2 reached equilibrium temperature at 240°C, 183°C and 210°C, respectively. The equilibrium temperature of C3 was significantly lower than that of B2 due to the addition of 25 wt.% CES. On the other hand, D2 had a higher equilibrium temperature than C3 due

to its 10 wt.% epoxy resin content. Poor adhesion of A2 resulted in its inability to protect the steel plate during fire as shown in Figure 4.12.

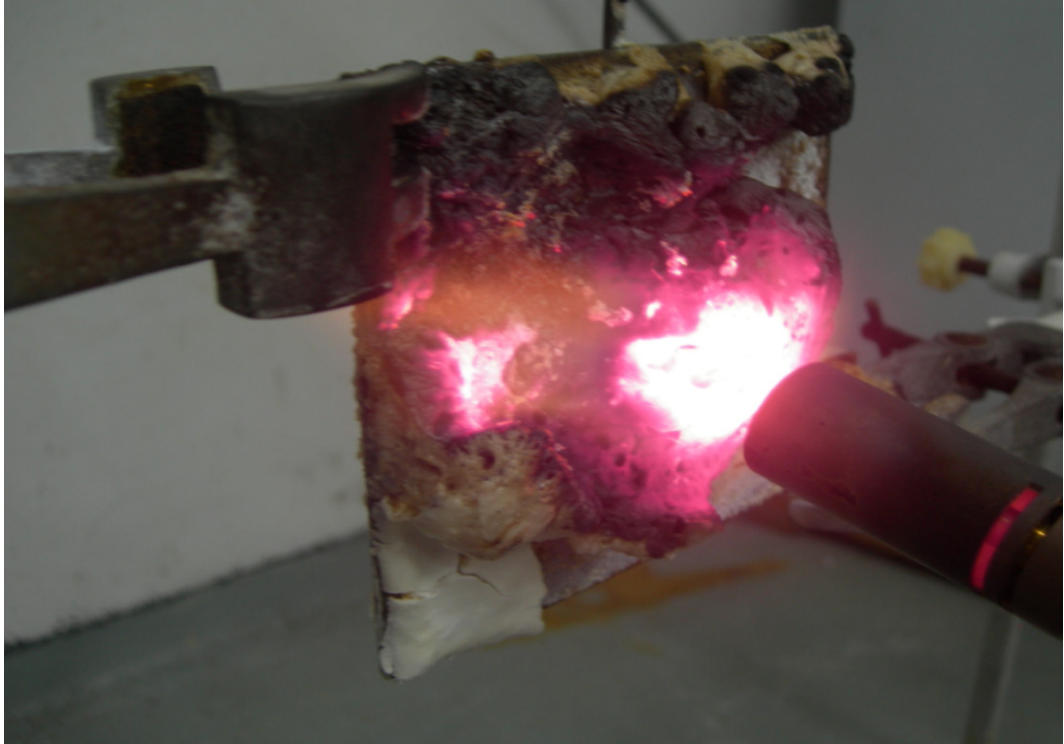


Figure 4.12 The steel plate coated with A2 formulation during fire test

Coating formulation A2 shows improved fire protection when compared to the uncoated steel with a failure time of 1 minute and 43 seconds. The improvement due to intumescence and charring was apparent, but some of the char detached from the plate during the experiment. The detachment could be explained by the loss of adherence of the coating to the plate because of its lightness and porosity, or by a loss of cohesion of the char. It could also be due to the effect of gravity, since the tests were carried out vertically. Hence, AMP formulation by itself has poor adhesive properties during fire.

AMP formulation is an interesting ‘active’ intumescent ingredient because the acid source (APP II) breaks down to yield a mineral acid, which then takes part in the

dehydration of the carbonization source (PER). This produces the carbon char and finally, the blowing agent (MEL) decomposes to yield gaseous products, improving the swelling. The latter causes the char to swell and produce the insulating multi-cellular protective layer (Duquesne et al., 2004).

Coating formulation B2 (A2+10 wt.% SF) showed improvement in fire protection performance compared to the AMP coating whereby the critical temperature was not reached after exposure to 90 minutes of fire and the equilibrium temperature reached was 250°C. The addition of 10 wt.% SF to formulation A2 resulted in excellent adhesion onto the plate and showed improvement in thermal destabilization of the intumescent coating as shown in Figure 4.13 (Jimenez et al., 2009; Wang and Shi, 2006). Development of intumescence was also observed and the char permits continuous adhesion between the coating and steel plate, providing longer-lasting protection. This char combines the positive effect of AMP and SF, promoting adhesion to the steel and producing a very hard char while ensuring the formation of a uniform foam structure (Wang and Yang, 2010). This suggests that physical and chemical interactions have occurred, resulting in the superior mechanical resistance of the char as well as its adhesion on the steel plate.

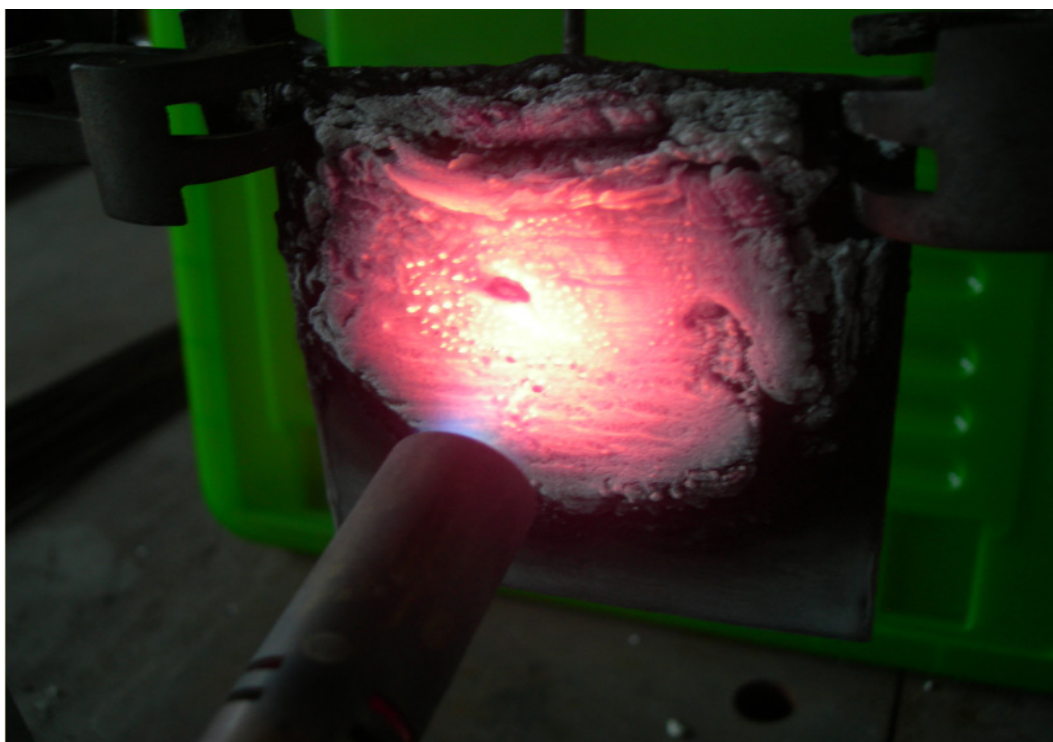


Figure 4.13 The steel plate coated with B2 formulation during fire test

Coating formulation C3 (B2+25 wt.% CES) displayed the best result in fire protection performance, where the critical temperature was not reached and the equilibrium temperature was just 183°C. Moreover, it exhibited the greatest expansion of char layer as shown in Figure 4.14. The swelling can potentially be initiated by the formation of a cohesive structure during burning, which could trap the degradation products into the residue and induce the swelling. This protective char limits the heat transfer from the heat source to the substrate, resulting in conservation of the underlying material. This mechanism protects structural steel in the event of a fire. Addition of 25 wt.% CES to formulation B2 produces an intumescent char that adheres strongly to the plate, exhibiting a regular hemisphere shape after the test. This shows that the addition of 25 wt.% CES resulted in optimum physical and chemical interactions.



Figure 4.14 The steel plate coated with C3 formulation during fire test

Coating formulation D2 (C3 +10 wt.% ER) was not as effective as C3 alone. Even though the critical temperature was not reached, the equilibrium temperature was higher at 210°C. This may be due to physical and chemical interactions that were not as efficient as in C3, leading to a char layer that was not as thick as the char layer formed by C3. This in turn resulted in a less effective protection of the steel plate. Addition of 10 wt.% of ER to sample C3 also produces an intumescent char that adheres strongly to the plate, exhibiting a regular hemisphere shape after the test (Figure 4.15) . In the next section, the bonding strength of AMP+SF+CES+ER formulations system were investigated by Instron microtester in order to better explain their mechanical properties.

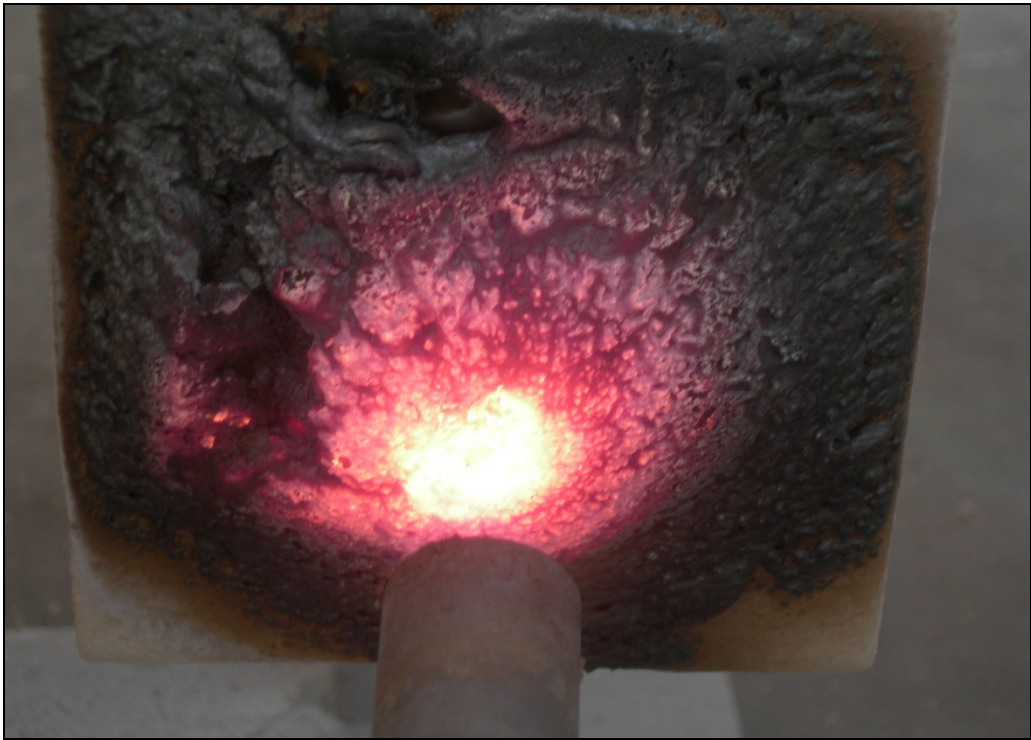


Figure 4.15 The coated steel plate with D2 formulation during fire test

4.4.5 Evolution of Fire Performance Using Small Scale Furnace Test

Temperature variations of the protected and unprotected steel plates obtained from experimental work during the heating and cooling phases was compared to the furnace and Eurocode fire curves (EC1, 2002) (Figure 4.16). The furnace temperature was controlled to closely follow the Eurocode parametric standard temperature-time curve. The steel plate protected with AMP+10 wt.% SF+25 wt.% CES (sample C3) intumescent fire protective coating experienced a lower rate of initial temperature rise than the unprotected steel plate. Also, the difference between the temperatures of the protected and unprotected steel plate increased to almost 450°C after about 22 minutes.

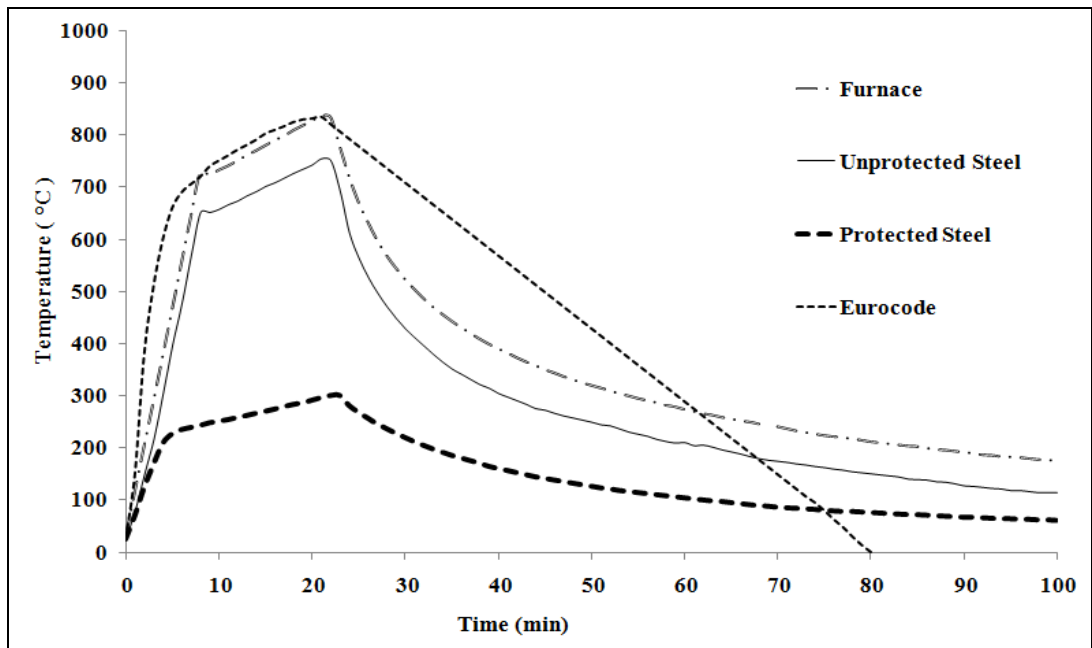


Figure 4.16 Time-temperature curves of protected and unprotected steel plates

The furnace test results show that the steel plate with fire protection could maintain its integrity and properties because the steel did not reach its critical temperature (Figure 4.17 (a)). However, the unprotected steel was deformed due to loss of strength and stiffness (Figure 4.17 (b)).

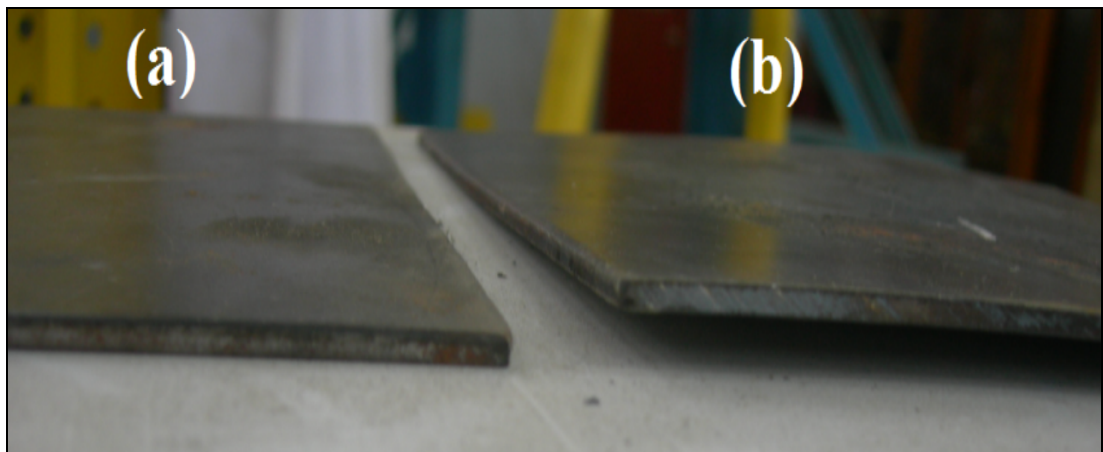


Figure 4.17 Deformation of the steel plates after fire test (a) protected and (b) unprotected

The steel coated with formulation C3 (AMP+10 wt.% SF+25 wt.% CES) formed an insulating protective multi-cellular layer (thickness 36.4 mm) upon heating (as

shown in Figure 4.18), which acts as a thermal barrier that effectively protects the substrate against fire. The formulation of these coatings were modified to study their physical and chemical properties to form an efficient protective char. Characteristics of this intumescent coating formulation include low amount of smoke, low toxicity and high degree of adhesion to the substrate.

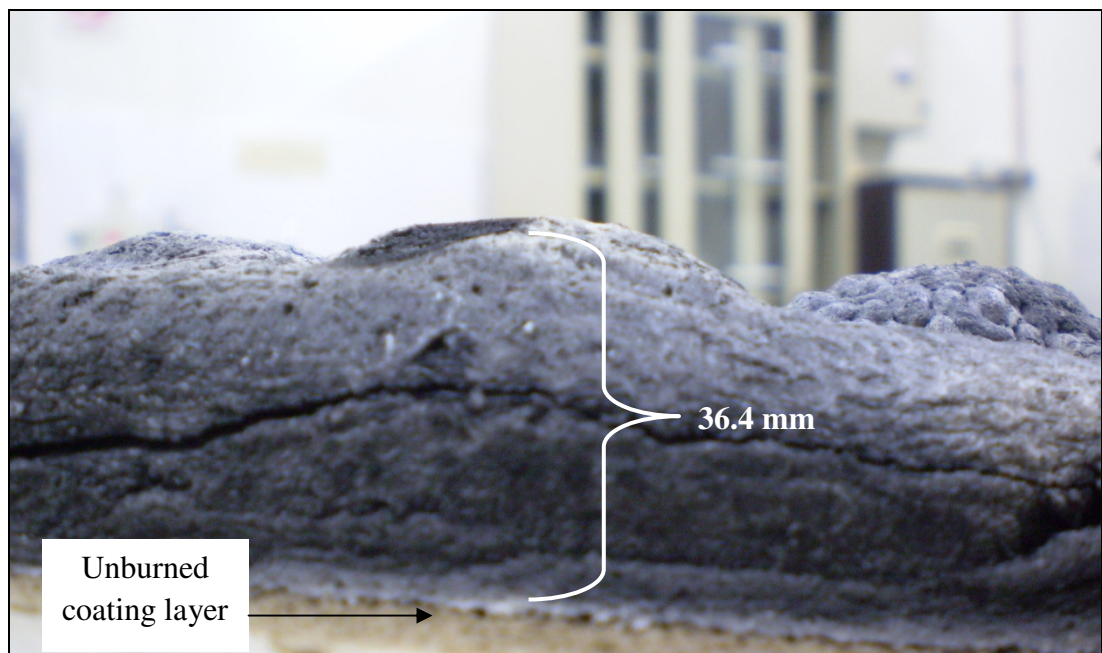


Figure 4.18 Residues obtained after the furnace test

Intumescent fire protective coatings are designed to provide an insulating barrier between flames and steel and are necessary to ensure the structural performance of the steel members at the temperatures anticipated during a fully developed fire. For coatings to be effective during crisis conditions, two unique characteristics are critical, the expansion of the coating, and the retention of the insulating char layer on the structure. The mechanism of intumescence is usually described as follows: first, the acid source breaks down to yield a mineral acid, then it takes part in the dehydration of the carbonization agent to yield the carbon char, and finally the blowing agent decomposes to yield gaseous products. The latter causes the char to

swell and hence provides an insulating multi-cellular protective layer. At the same time, this shield limits the heat transfer from the heat source to the substrate and the mass transfer from the substrate to the heat source resulting in conservation of the underlying material (Jimenez et al., 2006).

With such intumescent coatings, the burning coating as a block consisting of several separate layers can be visualised. The top char layer is followed by the intumescent front where the foaming reactions take place. Below is an unburned coating layer that still contains the flame retardant. The bottom layer represents the substrate that is being protected by the intumescent coating. The char-foam provides a physical barrier to heat and mass transfer, and therefore interferes with the combustion process (Gilman and Kashiwagi, 1997).

The Bunsen burner and furnace tests are useful because they enable observation of the changes during fires. However, they do not give further information on the effect of the flame retardant components on the surface morphology and thermal degradation of the intumescent coatings. Further investigation on selected intumescent coating formulations were carried out in detail using small scale lab test (TGA, SEM and FESEM) to better explain and compare their behavior and properties in a fire.

4.5 Thermal Analysis of Intumescent Coatings

In this part of the research, thermal analysis was carried out to study and compare the influence of SF binder, CES filler and different composition of epoxy binder on the different intumescent coating systems (B2, C3 and D1-D4) were compared and studied.

4.5.1 Influence of Silica Fume as Binder

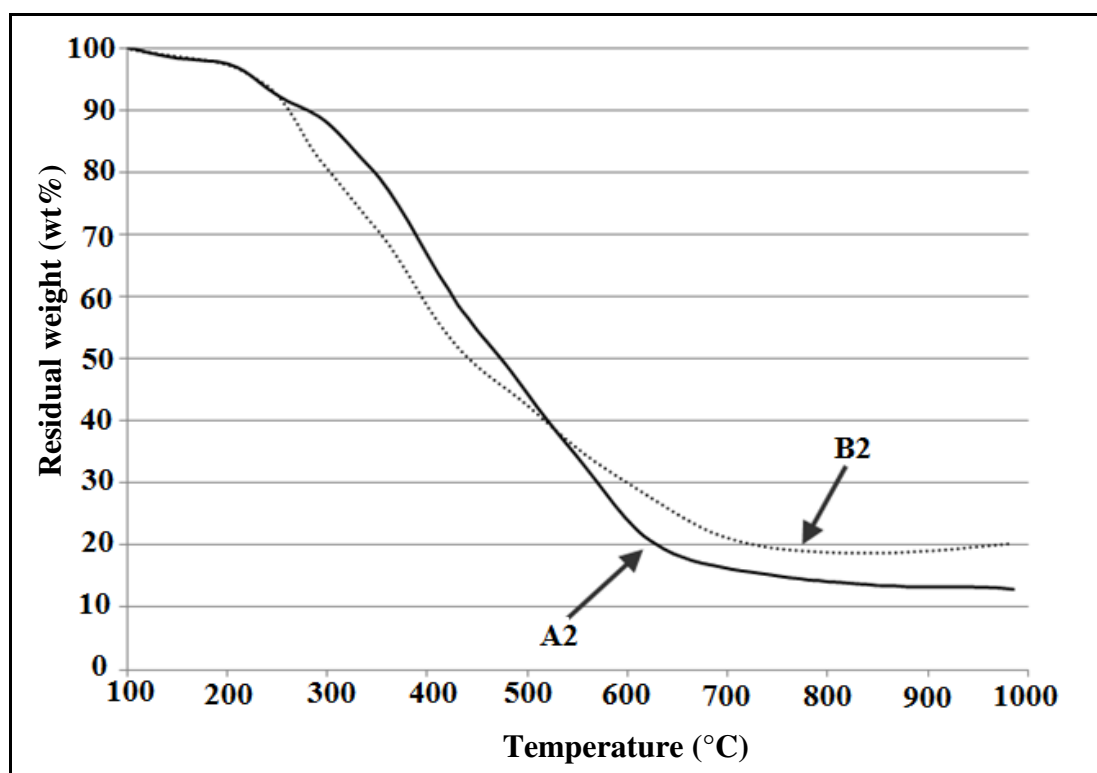


Figure 4.19 TGA curves of samples A2 and B2

The thermal stability of samples A2 and B2 was analyzed by using TGA as shown in Figure 4.19. The curves of the coatings were similar between 100°C to 250°C and the weight loss of each coating was less than 10 wt.% at 250°C. When the temperature was higher than 250°C, the TGA curves of the coatings became slightly different from each other. The TGA curve of B2 demonstrated that the residual weight of the coating was increased by the addition of SF. The residual weight of A2 and B2 at 750°C was 15.4 wt.% and 20.4 wt.%, respectively. The higher residual weights of B2 indicated that addition of 10 wt.% of SF content could enhance anti-

oxidation and thermal stability of the coatings, resulting in a good fire protection performance.

4.5.2 Influence of CES as Filler

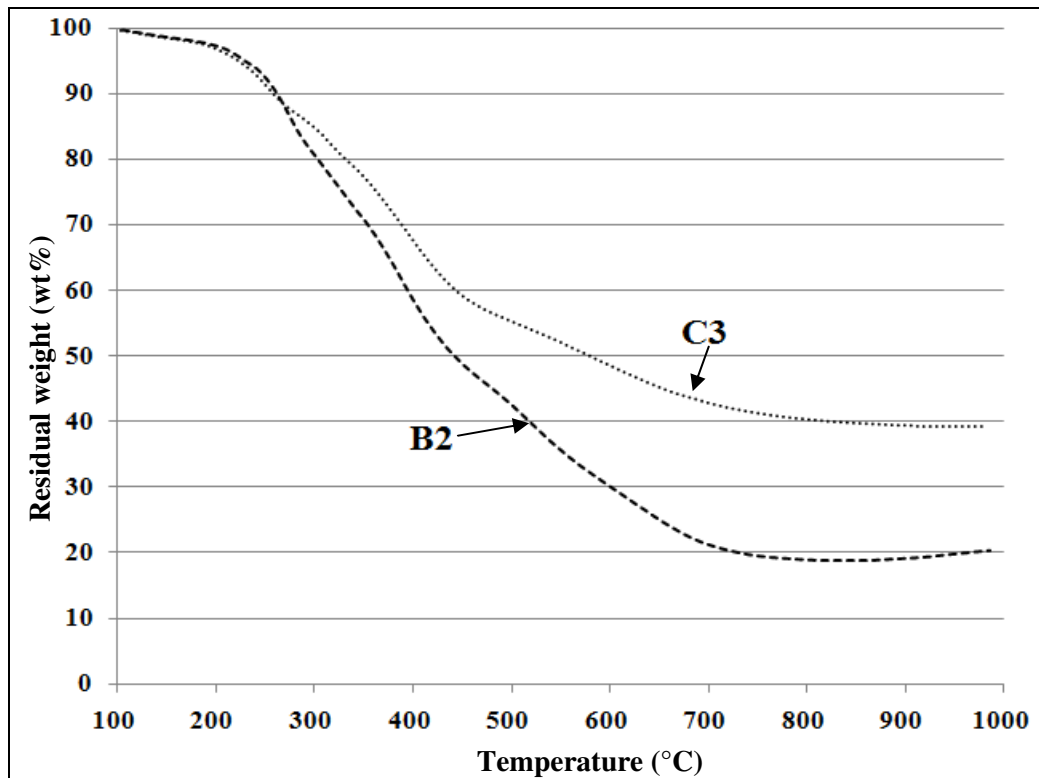


Figure 4.20 TGA curves of samples B2 and C3

The thermal stability of samples B2 and C3 was analyzed by TGA curves as shown in Figure 4.20. The curves of the coatings were similar between 100°C to 250°C and weight loss of each coating was less than 10 wt.% at 250°C. When the temperature was higher than 250°C, the TGA curves of the coatings became slightly different from each other. The TGA curves of C3 demonstrated that the residual weight of the coating was increased by the addition of 25 wt.% CES. The residual weight of B2 and C3 at 750°C was 20.4 wt.% and 40 wt.%, respectively. The higher residual weight of C3 indicated that 25 wt.% of CES content could enhance anti-oxidation and thermal stability of the coating as well as increase the fire protection performance.

4.5.3 Influence of Epoxy Resin

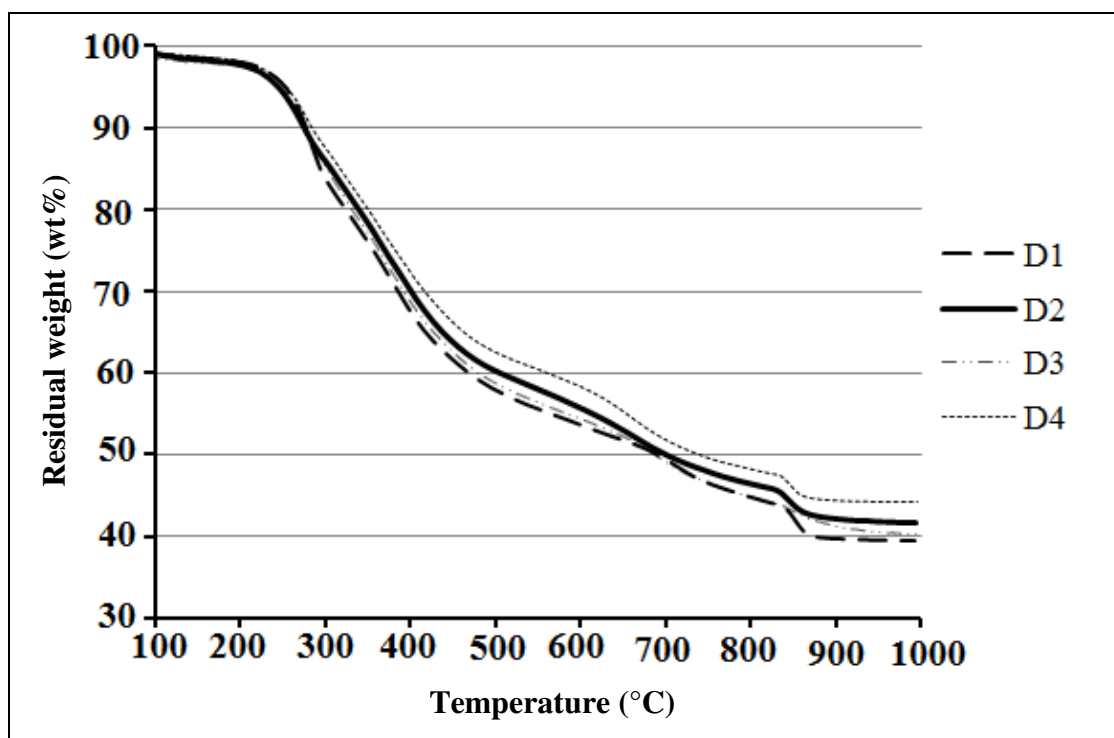


Figure 4.21 TGA curves of samples D1, D2, D3 and D4

TGA curves of the AMP+SF+CES+ER intumescent coatings system were presented in Figure 4.21. The curve profiles of the coatings were similar and the weight loss of each coating was less than 60 wt.%. The TGA curves demonstrated that the residual weight of all samples were increased with the increase of epoxy content in the temperature range of 30°C to 1000°C except for sample D2. The residual weight of D1, D2, D3 and D4 at 850°C was 41.8 wt.%, 43.5 wt.%, 42.7 wt.% and 45.2 wt.%, respectively. The residual weight of D2 (10 wt.% ER) was higher than D3 (15 wt.% ER) and this indicates that the optimal combination of 10 wt.% of epoxy content with flame retardant additives, SF and CES could enhance the anti-oxidation, thermal stability and fire protection performance of the intumescent sample.

4.6 Surface Morphology of Intumescent Coatings

In this study, the morphology of the coating and the char layers as well as the distribution of the cell size was characterized by SEM and FESEM images.

4.6.1 Influence of Binder and Filler

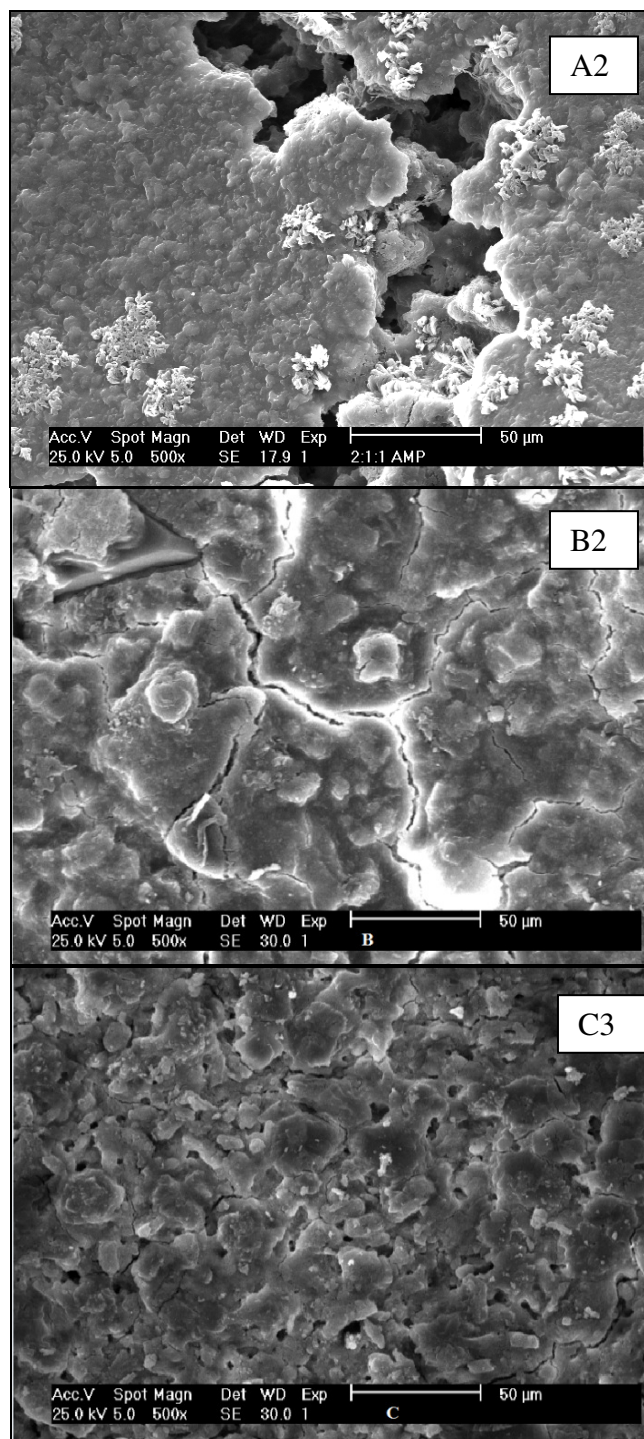


Figure 4.22 SEM micrographs of A2, B2 and C3 coatings

The efficiency of surface coatings depend strongly on its physical structure (Wang et al., 2006). The SEM micrographs of samples A2, B2 and C3 were shown in Figure 4.22. Sample C3 had a denser surface structure compared to samples A2 and B2. This surface structure could isolate the steel substrate from heat and fire and provide improved fire protection. Samples A2 and B2 showed some cracks on their surface structures. Cracks in the surface may result in heat and fire transfer to the steel substrate, which could lead to a decline of fire protection of samples A2 and B2. As a conclusion, sample C3 exhibited better fire protection performance compared to sample A2 and B2.

4.6.2 Influence of Epoxy Resin

The FESEM micrographs of the foam structure marked as D1 to D4 are shown in Figure 4.23. The porosity of the surface structure of samples D1, D3 and D4 was clearly visible. The char layer of sample D1 had a porous and tiny foam structure. The tiny foam structure could insulate the steel substrate from heat and fire. However, heat and fire may be transferred to the steel substrate through the porous foam structure that is porous, which could lead to a reduction of the fire protection of sample D1. The char layers of sample D3 and D4 showed agglomeration and coalescence of the foam structure, with sample D4 having a greater level of agglomeration and coalescence due to the increased epoxy content. The results indicate that the agglomeration of the foam structure of D3 and D4 were not uniform and porous, which could increase the rate of heat transfer and reduce the efficiency of fire protection. The dense foam structure of sample D2 was uniform and less porous. This foam structure is able to insulate the steel substrate from fire and provide better fire protection (Yew and Ramli Sulong, 2011). The efficiency of the char layers depend strongly on its physical foam structure (Wang et al., 2006).

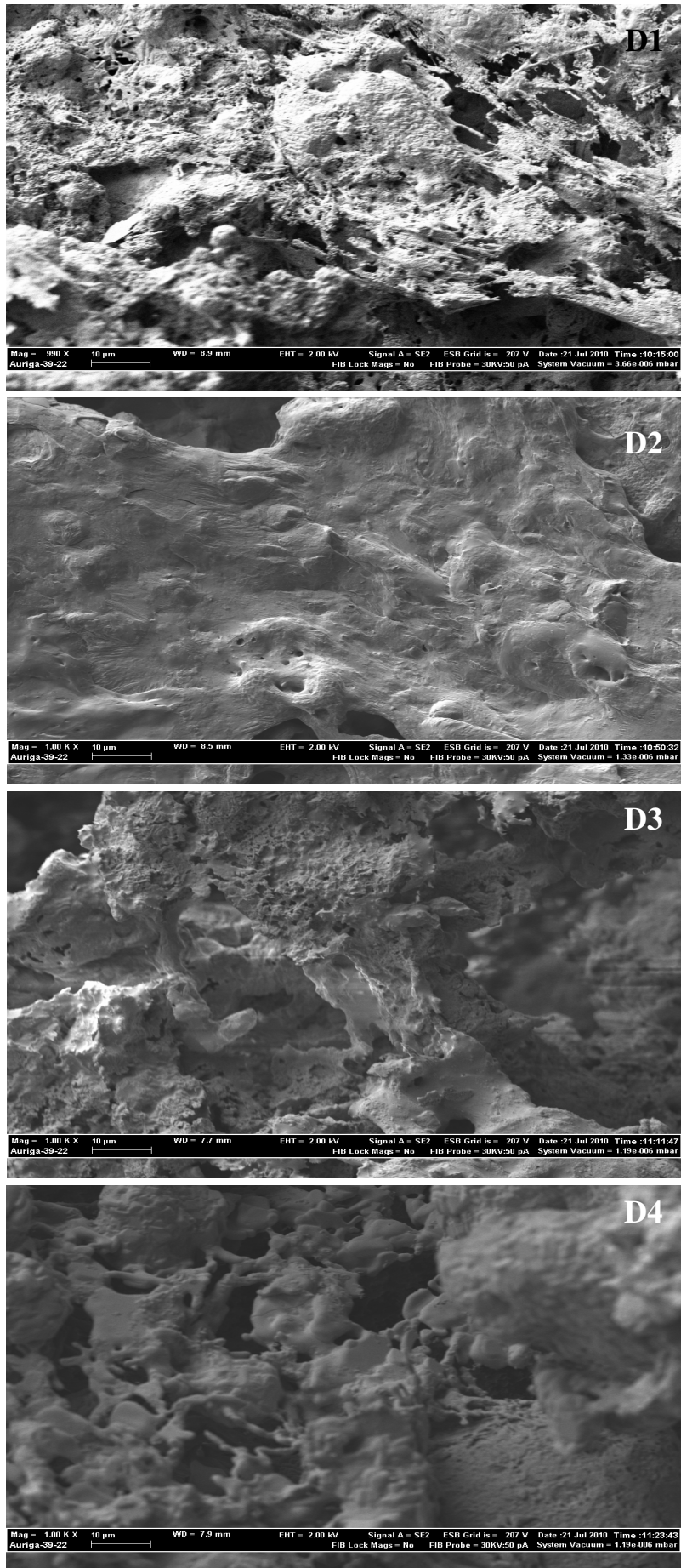


Figure 4.23 FESEM micrographs of the foam structure of D1, D2, D3 and D4

4.7 Bonding Strength of Intumescent Coatings

The bonding strength of the AMP+SF+CES+ER coating system was investigated using the Instron microtester. The bonding strength results only test for samples D1-D4 in the second part of the study as mentioned in the chapter one. The mechanical properties of the coatings are listed in Table 4.6.

Table 4.6: Mechanical properties of coatings

Sample	Crack charge, F (N)	Sticking area, A (m ²)	Bonding strength, f_b (Nm ⁻²)
D1	318.68	0.25×10^{-2}	0.13
D2	365.72	0.25×10^{-2}	0.15
D3	531.06	0.25×10^{-2}	0.21
D4	686.54	0.25×10^{-2}	0.28

The improvement in bonding performance was only compared among samples containing epoxy because epoxy is the main binder in this study. The coatings with different weight percent of epoxy (D1=5 wt.%, D2=10 wt.%, D3=15 wt.% and D4=20 wt.%) were tested and the results showed that bonding strength was clearly enhanced with the increase of epoxy binder content. It can be concluded that the increase of epoxy content is proportional to the improvement in the mechanical properties of the coating without much reduction of fire-resistant properties. The photos for each coating sample after the bonding test are shown in Figures 4.24, 4.25, 4.26 and 4.27. The images below show the plate coated with epoxy glue on the left and the plate coated with intumescent coating on the right.

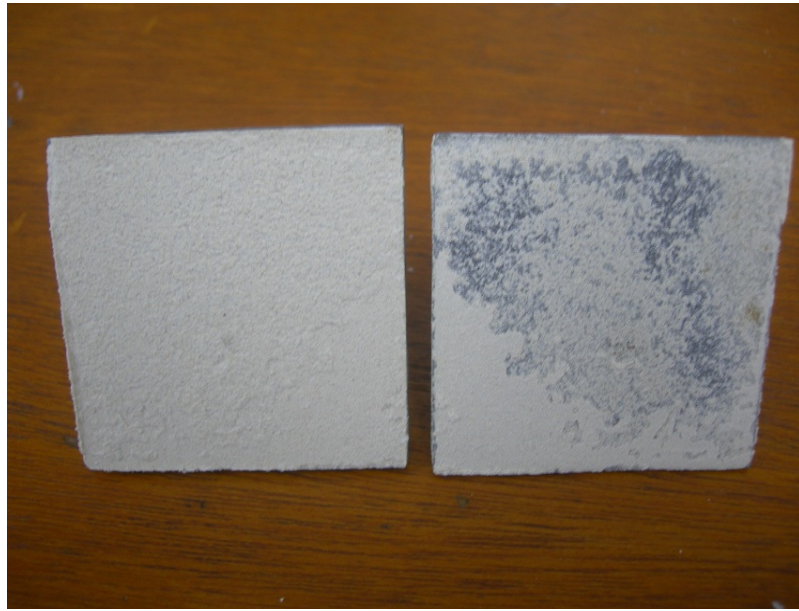


Figure 4.24 Coating sample D1 with 5 wt.% ER

Coating sample D1 with only 5 wt.% epoxy binder resulted in poor adhesion with most of the coating pulled off, exposing the steel plate beneath. The bonding strength between the coating and substrate was merely 0.13 MPa.



Figure 4.25 Coating sample D2 with 10 wt.% ER

The coating with 10 wt.% epoxy binder (D2) showed better adhesion compared to 5 wt.% epoxy binder (D1), with reduced detachment of the coating. The results showed

that the bonding strength between coating sample D2 and the substrate achieved 0.15 MPa, which is a 15.38 % improvement in bonding strength compared to sample D1.



Figure 4.26 Coating sample D3 with 15 wt.% ER

Coating sample D3 with 15 wt.% epoxy binder showed good adhesion to the steel plate, with significantly less detachment of the coating compared to the previous samples as shown in Figure 4.26. Bonding strength of sample D3 achieved 0.21 MPa. Addition of 15 wt.% epoxy content resulted in 40 % improvement of bonding strength compared to sample D2.



Figure 4.27 Coating sample D4 with 20 wt.% ER

Coating sample D4 with 20 wt.% epoxy binder showed excellent adhesion, with even and strong bonding of the coating to the steel plate. The results showed that the bonding strength achieved 0.28 MPa which is an increment of 33.33 % compared to sample D3. There was only slight detachment of the coating as shown in Figure 4.27. It can be concluded that the coating formulation is stable and resistant to detachment from the steel surface.